

Using a surrogate contact pair to evaluate polyethylene wear in prosthetic knee joints

Anthony P. Sanders,^{1,2} Carly A. Lockard,² Joel N. Weisenburger,³ Hani Haider,³ Bart Raeymaekers²

¹Ortho Development Corp., 12187 Business Park Dr., Draper, Utah 84020

²Department of Mechanical Engineering, University of Utah, 50 S. Central Campus Dr., MEB 2122, Salt Lake City, Utah 84112

³Department of Orthopaedic Surgery and Rehabilitation, University of Nebraska Medical Center, 985360 Nebraska Medical Center, Omaha, Nebraska 68198-5360

Received 22 May 2014; revised 30 October 2014; accepted 9 December 2014

Published online 00 Month 2015 in Wiley Online Library (wileyonlinelibrary.com). DOI: 10.1002/jbm.b.33360

Abstract: With recent improvements to the properties of ultra-high molecular weight polyethylene (UHMWPE) used in joint replacements, prosthetic knee and hip longevity may extend beyond two decades. However, it is difficult and costly to replicate such a long *in vivo* lifetime using clinically relevant *in vitro* wear testing approaches such as walking gait joint simulators. We advance a wear test intermediate in complexity between pin-on-disk and knee joint simulator tests. The test uses a surrogate contact pair, consisting of a surrogate femoral and tibial specimen that replicate the contact mechanics of any full-scale knee condyle contact pair. The method is implemented in a standard multi-directional pin-on-disk wear test machine, and we demonstrate its application via a two-million-cycle wear test of three different UHMWPE formulations. Further, we demonstrate the use of digital photography and image processing to accurately quantify fatigue damage based on the reduced transmission of light through a damage area in a UHMWPE specimen. The

surrogate contact pairs replicate the knee condyle contact areas within $-3%$ to $+12%$. The gravimetric wear test results reflect the dose of crosslinking radiation applied to the UHMWPE: 35 kGy yielded a wear rate of 7.4 mg/Mcycles, 55 kGy yielded 1.0 mg/Mcycles, and 75 kGy (applied to a 0.1% vitamin E stabilized UHMWPE) yielded 1.5 mg/Mcycles. A precursor to spalling fatigue is observed and precisely measured in the radiation-sterilized (35 kGy) and aged UHMWPE specimen. The presented techniques can be used to evaluate the high-cycle fatigue performance of arbitrary knee condyle contact pairs under design-specific contact stresses, using existing wear test machines. This makes the techniques more economical and well-suited to standardized comparative testing. © 2015 Wiley Periodicals, Inc. *J Biomed Mater Res Part B: Appl Biomater* 00B: 000–000, 2015.

Key Words: wear, UHMWPE, pin-on-disk, fatigue, testing, standards, knee replacement

How to cite this article: Sanders AP, Lockard CA, Weisenburger JN, Haider H, Raeymaekers B. 2015. Using a surrogate contact pair to evaluate polyethylene wear in prosthetic knee joints. *J Biomed Mater Res Part B* 2015;00B:000–000.

INTRODUCTION

Significant progress has been made to improve the mechanical properties of ultra-high molecular weight polyethylene (UHMWPE) and to reduce its susceptibility to oxidation that limits its longevity in joint replacement applications. In parallel, implant bearing development practices must ensure that next-generation implants will fulfill the expectation of improved durability. In the United States, current life expectancy at age 65, which is the average age of patients receiving joint replacement surgery, is >17 years.¹ However, the current practice of implant wear testing in knee and hip joint simulators^{2,3} is to limit the tests to 5 million cycles, which is commensurate with 2–5 years of service dependent on patient activity level.^{4,5} Although imperfect, these sophisticated tests⁶ provide the most clinically relevant *in vitro* means of implant durability evaluation because they mimic the complicated motion of the knee during walking gait. Rou-

tinely extending the tests beyond the current practice of 5 million cycles is prohibitively expensive, and often, unproductive if it merely extends evidence of an established linear wear trend. Basic wear tests such as pin-on-disk (POD) tests have the advantage of using simple specimens and equipment,⁷ which makes them well-suited for long-term durability tests of the material only and not the whole implant system. However, the contact geometry of the specimens and the imposed loading and kinematics typically bear little resemblance to those of implants, which diminishes the relevance of the tests to specific implant designs and to the clinical scenario. Intermediate approaches that balance complexity with clinical relevance have been developed,^{8,9} but their typical use has been for comparative tests in which the superiority of new UHMWPE formulations has been shown in short durations (<2 million cycles). Such intermediate approaches may be essential to cost-effective testing

Correspondence to: A. P. Sanders; e-mail: tsanders@odev.com
Contract grant sponsor: Ortho Development Corp.

that is commensurate with anticipated implant durability extending to two decades or longer.

In addition, several research articles^{10–17} have evaluated wear performance of UHMWPE knee implants using approaches that are less complicated than knee simulators and thus are potentially suited to less costly high-cycle, that is, >10 million cycles, durability testing. A few of these have incorporated geometric details of knee condyle design. This is valuable because different designs elicit different contact stresses under equivalent stances and loading.¹⁸ Several approaches have employed planar articulation of a rigid indenter with condyle-like, convex geometry against a flat UHMWPE test specimen. This configuration provides the advantage of low equipment complexity but the potential limitation that few total knee prostheses have convex-on-flat condyle designs. Van Citters et al. developed a multi-station, rolling-sliding test rig that articulated convex cylindrical specimens against each other, and they showed that the specimen geometry and loading yielded a contact stress field in the UHMWPE specimen similar to that of convex-on-flat condylar contact.^{15,19} To date, none of these approaches has evolved to become a widely adopted and standardized testing practice. Furthermore, primarily qualitative results have been reported on fatigue-evoked subsurface cracking that leads to spalling, which is sometimes called “delamination,” and is a common failure mode of tibial inserts. Although perhaps sufficient for comparing two different UHMWPE types differing greatly in fatigue resistance, such a non-quantitative approach would be inadequate for critically evaluating competing designs or materials with closer parity in their durability.

This article attempts to address this problem and describes a novel approach to testing knee prosthesis contact pairs for high-cycle durability, relevance to specific designs, and execution in widely installed, commercially available wear test equipment. The approach is based on designing a surrogate contact pair that replicates the contact area of any complicated contact pair to second-order accuracy.²⁰ We show the feasibility of this surrogate approach in the context of knee condyle contact pairs by using quasi-static contact tests to validate the accuracy of the surrogates compared with the original contact pairs they represent. Further, we use 2-million-cycle wear tests to demonstrate the practical application of surrogate contact pairs in an existing, widely available, multi-station wear test apparatus. The test evaluates a specific condylar design paired with three different types of crosslinked UHMWPE. Finally, we demonstrate a method of quantifying fatigue damage based on the reduced transmission of light through damage areas in a trans-illuminated UHMWPE wear specimen.

MATERIALS AND METHODS

Specimen design

Two separate original contact pairs [Figure 1(a), Table I] representing convex-concave condylar contact of a full-scale total knee prosthesis were designed. In the original distal (OD) pair, the convex member represented a distal segment from the femoral condyle, and in the original posterior (OP) pair, the convex member represented a posterior segment.

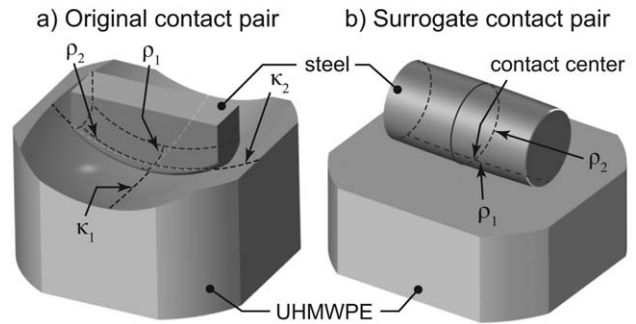


FIGURE 1. Schematics of contact pairs created for quasi-static contact tests.

The concave members in both original pairs were identical and represented the surface of a tibial condyle. The OD pair simulated condylar contact with the femur posed at a low flexion angle (e.g., 0°) such as in the highly frequent load bearing stance of the walking gait. The OP pair simulated condylar contact at a high flexion angle (e.g., 120°), such as would occur during squatting or sitting and rising from a chair. The concave members were made of UHMWPE, and the convex members were made of stainless steel to approximate the stiffness of cobalt-chromium (Co-Cr), which is the typical femoral implant material, at reduced expense. The contact surfaces of all of these original bodies were toroidal (Figure 1), as defined in more detail by two orthogonal, principal curvatures at their centers of contact (Table I). The specific forms and dimensions of the OD and OP contact pairs originated from a design of a contemporary full-scale, posterior-stabilized, total knee prosthesis, yet the forms and dimensions were altered slightly to maintain generality and to protect proprietary design details.

To correspond with each original contact pair, a separate surrogate contact pair [Figure 1(b)] was designed: a surrogate distal (SD) pair and a surrogate posterior (SP) pair. Each of these contact pairs consisted of a steel spheroid (or segment thereof) mated with a flat UHMWPE disk. The principal curvatures of each spheroid (Table I), at the point of initial contact, were computed from the principal curvatures of the original contact pair following our previously developed theory for designing a surrogate contact pair.²⁰ According to the theory, the surrogate pair will generate a contact area that replicates, to second-order accuracy, the contact area of the original pair it represents when both pairs are loaded identically. The theory was previously validated with members made of a stiff polymer (ULTEM™, polyetherimide)²⁰ and of ceramic and Co-Cr.²¹

The steel specimens were manufactured on a CNC lathe and polished to a roughness of $R_a = 40\text{--}50$ nm. The concave UHMWPE specimens were machined using a custom-ground milling cutter in a CNC mill, following a common technique for tibial implants. The flat UHMWPE specimens were machined using a diamond-lapped tool in a fly-cutter. The average roughness of the UHMWPE contact surfaces was $R_a = 700\text{--}800$ nm, and they were oriented perpendicular to the compression-molding direction of the raw material.

TABLE I. Principal Curvatures (mm^{-1}) of the Specimens at Their Initial Contact Points

Femoral Condyle Segment Represented	Original		Surrogate	
	Convex (ρ_1, ρ_2)	Concave (κ_1, κ_2)	Convex (ρ_1, ρ_2)	Flat ^a
Distal	0.0345, 0.0582	0.0111, 0.0325	0.0180, 0.00195	0, 0
Posterior	0.0345, 0.2669	0.0111, 0.0325	0.1223, 0.00195	0, 0

Symbols per Figure 1.

^aCurvatures of Surrogate “concave” specimens were zero because the specimens were flat.

Several quasi-static contact tests and a single wear test were performed using the four contact pair designs, with several different UHMWPE types, as summarized in Table II and elaborated in the following sections.

Quasi-static contact tests

Experiments were performed to compare the contact areas of the original and surrogate contact pairs, with their mating surfaces pressed together under a normal load in a uniaxial, electro-mechanical test frame (ELF 3300, Bose, USA). For each contact pair, one test applied a normal load increasing from 0 to 1,000 N in 1 s and subsequently unloaded back to 0 N in 1 s. A second test applied the same normal loading in 100 s and unloading in 100 s. The different test durations of 2 s and 200 s provided validation of the surrogates taking into account the viscoelastic properties of UHMWPE. A previously detailed “fingerprinting” technique²¹ was used to record the contact area between the stainless steel and UHMWPE specimens. Alignment of the specimens ensured that first contact occurred on the apices of both bodies for the original pairs, and on the apex of the spheroid for the surrogate pairs. The resulting contact area was digitally photographed at 40 \times magnification with an optical coordinate measuring machine (Nexiv VMR 3020, Nikon, Japan) and measured to determine its major and minor diameters and its area.

POD wear tests

Wear experiments were performed with SP pairs in a multi-station, 2D planar POD apparatus (OrthoPOD, AMTI, USA), applying a high-stress scenario meant to elicit spalling fatigue in the UHMWPE specimen. Six identical steel spheroidal specimens were fabricated; each was adapted with a

welded stem for fixation in the test machine. Six 7-mm-thick UHMWPE disk specimens, with two in each of the γ +N₂, XL, and VEXL types (described in Table II) were aged for 2 weeks according to ASTM F 2003. Each contact pair was articulated along a square path of approximately 10 \times 10 mm (see dash-dot line in Figure 2) at a typical 1 Hz gait frequency. Serum lubricant (20 g L⁻¹ protein per ISO 14243-1) which was exchanged at intervals of 500 k cycles. A 300N normal load was used, to elicit a maximum contact pressure of \sim 32–37 MPa approximated using Hertzian contact theory. Because the contact area between the specimens was elliptical, the square wear track yielded a central region with overlapping contact areas from two opposite sides of the track, which was subject to multi-directional, reversed sub-surface shear stresses in the disk. Wear of each specimen was measured gravimetrically (ISO 14243-2) at two intervals, corresponding with the data points in Figure 7. The wear scars on the UHMWPE disks were examined with a stereomicroscope (10–40 \times) in reflected and transmitted light to detect subsurface damage.

Potential subsurface damage was detected and closely examined on a single radiation-sterilized specimen. The damage area was quantified by measuring the regions of decreased light transmission, which are associated with damage to the UHMWPE, in photographic images of the trans-illuminated specimen. Figure 3(a) shows the experimental set-up. The POD specimen was back-lit using a fiber optic illuminator (Fiber-Lite, Bausch & Lomb, USA) and diffusing screen (0.007 mm matte two-sided film, Inventables, USA). The specimen was secured in a vise and was surrounded by opaque plastic sheeting to block light from

TABLE II. Use of Contact Pairs and UHMWPE Material Types

	Contact Tests	Wear Test	
Contact pairs	OD SD OP SP	SP	
UHMWPE types	Type 2, virgin	Type 1	γ +N ₂ XL VEXL

Type 1 = GUR® 1020, Celanese, Oberhausen, Germany.

Type 2 = GUR® 1050, Celanese, Oberhausen, Germany.

γ +N₂ = sterilized (25–40 kGy gamma radiation) in N₂-filled package.

XL = crosslinked by 55 kGy gamma radiation and re-melted.

VEXL = GUR® 1020E, Celanese, Oberhausen, Germany (GUR 1020 with 0.1% vitamin E), crosslinked by 75 kGy gamma radiation, not re-melted.

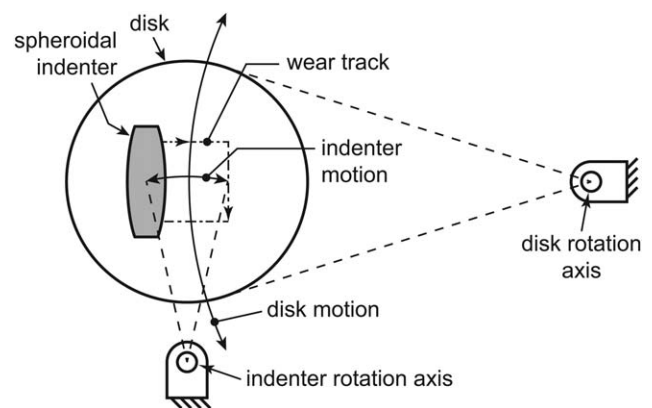


FIGURE 2. Schematic of a single station of the multi-station wear test (plan view), showing coordinated indenter and disk motions that create an \sim 10 \times 10 mm sliding path indicated by the dash-dot line with arrows showing the sliding direction (drawing not to scale).

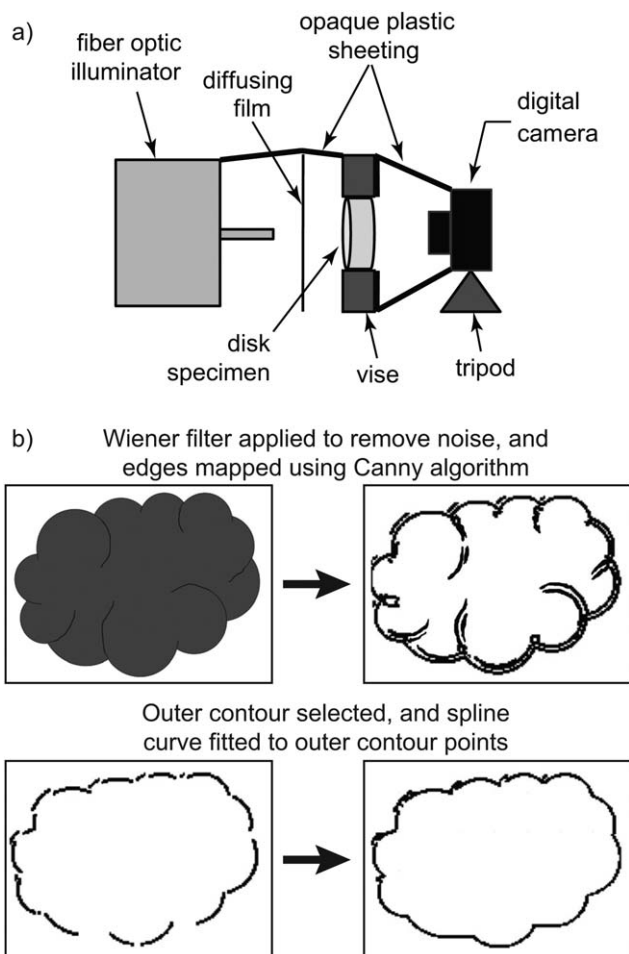


FIGURE 3. Set-up for image capture (a) and schematic of image processing (b) for fatigue damage area measurement.

passing around the edges of the specimen, as well as to block ambient light from entering the area between the fiber optic illuminator, the camera, and the POD specimen, as well as between the specimen and the digital camera.

Images were captured with a digital camera (Powershot ELPH 300 HS, Canon, USA) and digitally processed using the process illustrated in Figure 3(b). The images were filtered in Matlab using a Wiener filter and edge detection was subsequently performed using the Canny edge function. The resulting matrix of edge pixels was sorted into true damage edges and non-damage edges, caused by noise and regions of light saturation, based on a threshold of edge pixel density in the neighborhood surrounding each pixel. Edge pixel density was defined as the number of edge pixels (white pixels) divided by the total number of pixels (black and white pixels) in a given image area. The threshold density for damage versus non-damage was determined by first selecting representative damage and non-damage sample regions of the disk specimen (i.e., damage region exhibited visible damage and was within contact area; non-damage region was visually intact and outside of POD contact area). The maximum edge-pixel density from the non-damage sample region at the optimal sample size was used as the

threshold density for eliminating non-damage edge pixels. Once edge pixels outside of the damaged region were eliminated, the outermost remaining edge pixels were selected as representative of the damage region outline. A spline curve was fit to these outline pixels and the area within this spline curve was calculated to represent the area of the damage region. The damage area in pixels was then converted to mm^2 based on a captured scale image.

The damage region was also examined by obtaining topographic images of the test surface surrounding the region using a scanning white light interferometer (New-View 5000, Zygo, USA), and by sectioning through the region by sawing and then microtoming with a glass knife, before examining the exposed surface with optical and electron microscopy.

RESULTS

Quasi-static contact tests

Figure 4 shows that the contact area contours resulting from contact between the surrogate pairs were generally elliptical in shape. In the measured contact area, the surrogate pairs exhibited error in the range -12% to $+6\%$, and in the major diameter, the error was in the range -3% to $+7\%$ (Figure 5). The size of the contact area increased with the duration of the trials as a result of the viscoelastic properties of UHMWPE. Asymmetry in the contours from the original contact pairs resulted from a minor geometric form error in the disks' coronal radii, as illustrated in Figure 6.

Wear test and damage assessment

Figure 7 shows the gravimetric wear versus the number of gait cycles for the different UHMWPE materials. The two moderately crosslinked UHMWPE types (XL and VEXL) displayed similar wear rates (1.0 and 1.5 $\text{mg}/\text{Mcycles}$, respectively), which were lower than that of the conventional radiation-sterilized ($\gamma+\text{N}_2$) material (7.4 $\text{mg}/\text{Mcycles}$). The wear tracks created on the UHMWPE disks were similar in all specimens. A typical example is shown in Figure 8, also indicating the wear path followed during the POD experiment as a black dashed line. The odd shape of the wear damage was caused by overlapping of the elliptical contact area, and by the rotations applied by the test apparatus to approximate a square track (Figure 2). One radiation-sterilized specimen showed signs of subsurface damage that

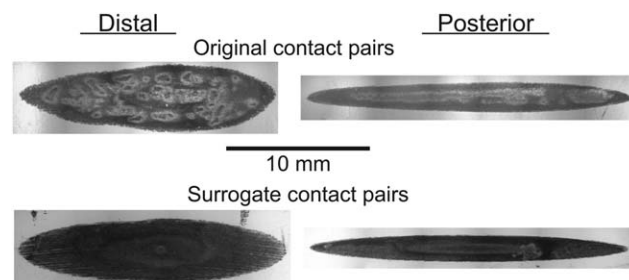


FIGURE 4. Example contact areas from quasi-static contact tests, showing the close similarity between the areas generated by the original pairs and those generated by their counterpart surrogate pairs.

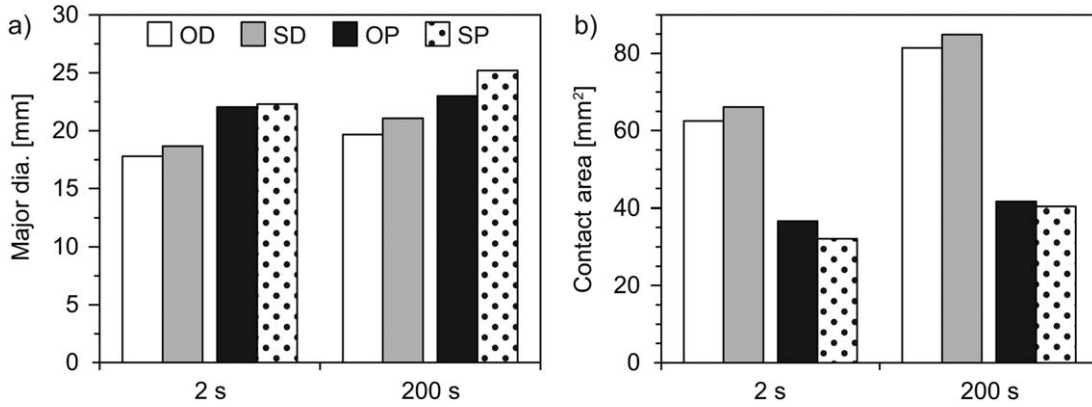


FIGURE 5. Quasi-static contact test results for 2 s and 200 s total test durations: (a) major diameter, and (b) contact area. Side-by-side bars compare corresponding original and surrogate contact pairs.

was detected under reflected light as a small, faintly whitened area. Under trans-illumination, the damage was more noticeable as a small darkened region.

Figure 9 shows an example of quantifying the damaged area of the UHMWPE specimen after the POD test. The damage region consisted of three distinct dark patches within an area of approximately 8×6 mm [Figure 9(a)]. Also, the wear track, which was starkly apparent under reflected light [Figure 8], was essentially invisible under trans-illumination [Figure 9(a)]. The image capture and processing techniques successfully isolated each patch and identified its edge contour [Figure 9(a)], resulting in contiguous perimeter spline fits [Figure 9(a)]. The areas of the three damage patches [from top to bottom in Figure 9(a)] were determined to be 1.347, 5.078, and 1.808 mm², respectively.

Figure 10 shows an optical micrograph of a cross-section of the UHMWPE specimen through the damage region, obtained by slicing the specimen. No evidence of cracking or other disruption is observed. Figure 11 displays the surface topography on the UHMWPE surface that articulated with the surrogate femoral specimen. The texture closely resembles the dark patches seen under trans-illumination. These observations suggest that the damage identified as dark patches was located very close to the surface of the UHMWPE specimen.

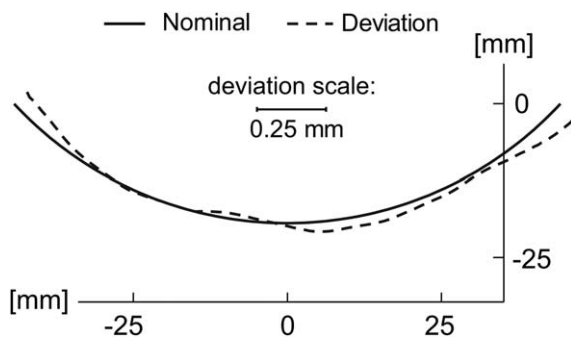


FIGURE 6. Typical graph of the coronal radius through the center of the concave disks used in both the OD and OP contact pairs, showing the nominal form (of a perfect radius) and the deviation of the actual specimen.

DISCUSSION

The first key result is the close correspondence between the contact areas of the original pairs and their counterpart surrogate pairs, with absolute error at a maximum of 12%, in both short (2 s) and long (200 s) duration quasi-static contact tests. UHMWPE is a viscoelastic material and Hertzian contact theory assumes that the materials are elastically deformed. Nonetheless, the surrogate pairs accurately mimicked the contact areas of the original pairs because the correspondence (between surrogates and originals) is based on the geometry of the mating surfaces rather than their material properties. Specifically, the surrogate pairs' surfaces replicated the separation between the original pairs' surfaces to second-order accuracy, with respect to distance from the initial contact point.²⁰ Hence, the viscoelastic nature of UHMWPE was not a limitation in the effectiveness of the surrogate specimens to simulate the contact area of the original specimens.

Two main sources of error might have influenced the contact tests. First, the form error in the concave UHMWPE disks (Figure 6) caused the contact area to be larger on one

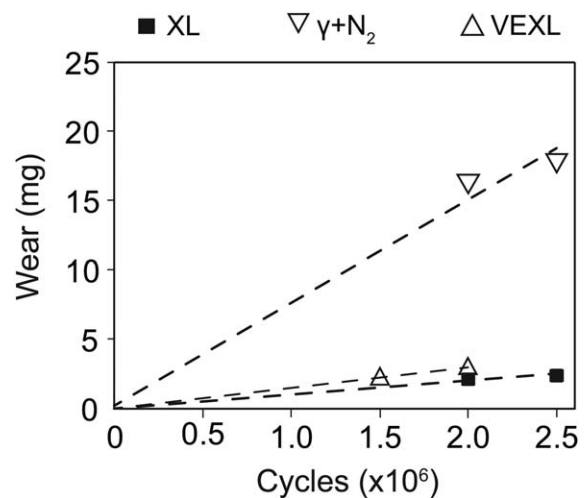


FIGURE 7. Gravimetric wear results with linear fits to emphasize the lower wear rates of the two moderately crosslinked materials.

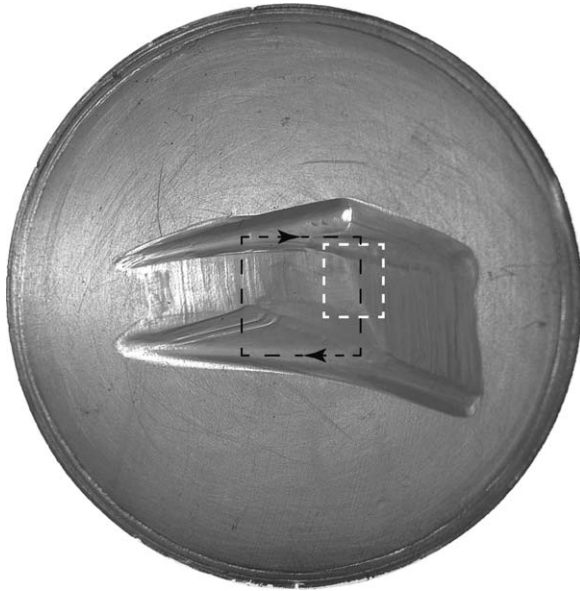


FIGURE 8. Typical wear track on UHMWPE disk from wear test. The black dashed line indicates the wear path of the centerpoint of the contact area. Evidence of subsurface damage was detected in one radiation-sterilized specimen in the white-bordered area.

side of the minor diameter than the other, creating asymmetry in the contact area of the original contact pair. Second, higher-order geometric discrepancies between the original and surrogate pairs could have contributed error. Because the surrogate theory is based on a second-order geometric approximation, the accuracy is inversely related to the contact area.²⁰

Verification of the accuracy of the trans-illumination-based damage area measurement method was provided via visual confirmation of a close correspondence among the digital images of the dark patches in the UHMWPE specimen, the detected edges of those patches, and the spline curves fit to the edges (Figure 9). The accuracy of the tech-

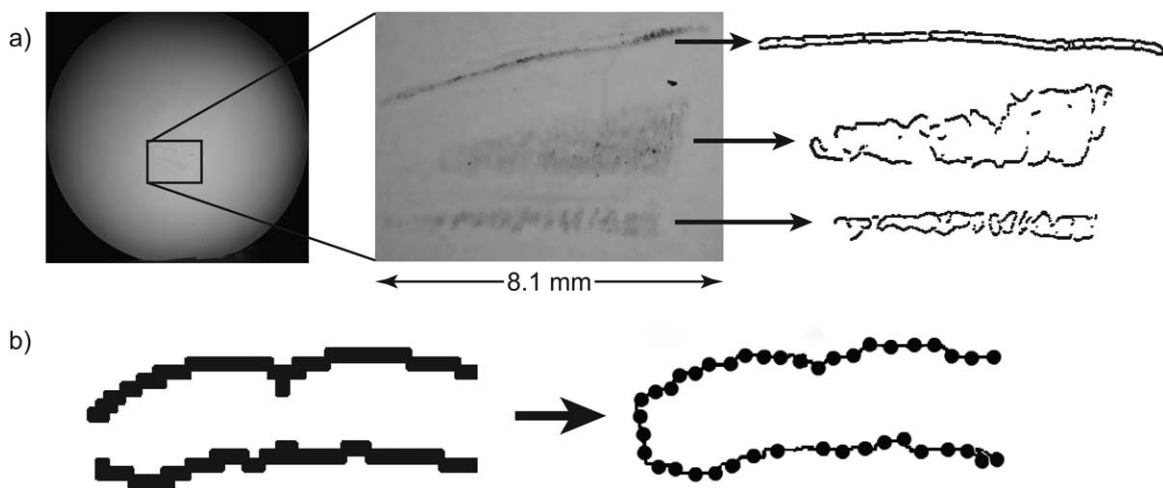


FIGURE 9. (a) Process of isolating the contours of the damage regions from digital photograph of disk specimen. (b) Example spline fit to damage contour for a portion of one of the three major damage regions (spline points in right image exaggerated for clarity).

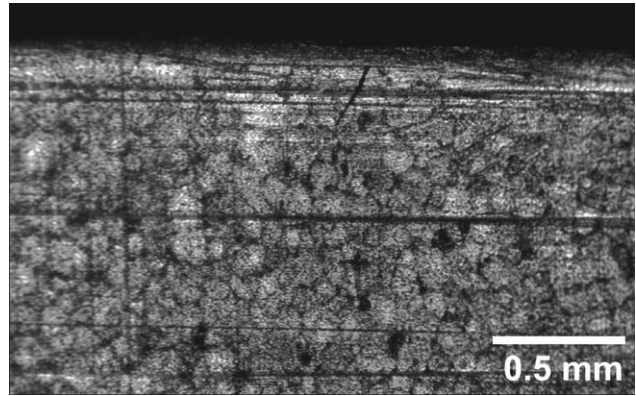


FIGURE 10. Optical micrograph (reflected light) of cross-section through the damage region, showing no evident disruption below the surface.

nique is affected most directly by the camera resolution and camera distance from the specimen, and it may be improved through the use of higher-resolution imaging equipment. Furthermore, the image quality is dependent on light level, light position relative to the damage region, and camera angle relative to the specimen. Each of these parameters requires manual adjustment to optimize the image quality for a particular specimen. Once the image is captured, the parameters for the Wiener filter and Canny edge detection must be tailored to each image. Poor image quality or processing parameters may lead to incorrect identification of damage versus non-damage regions, as well as inaccurate area contour detection and area measurement.

In addition, the damage area measured via this method was a projection of the true damage area onto the image plane. For damage such as a crack oriented obliquely to the specimen surface, the projected area would have been less than the actual area. In this particular case, the damage was confirmed to be near-surface via microscopic examination of a cross-sectional slice through the damage region, so error due to the projection effect was likely small.

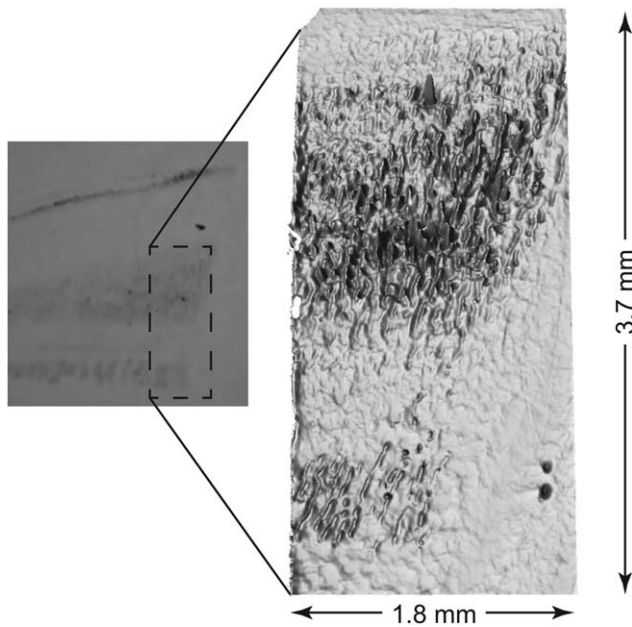


FIGURE 11. Surface topography of the UHMWPE specimen obtained with white light interferometry (right), with reference to the dark patches photographed under trans-illumination [from Figure 9(a)]. Topographic height is exaggerated relative to the lateral dimensions of the image; average roughness is $R_a = 13.7 \mu\text{m}$ and peak-to-valley is $76.0 \mu\text{m}$.

This present method improves upon image-based damage measurement methods used in previous research, which either used back-lit images only for simple confirmation and illustration of damage²² or relied on hand-tracing to find the contours of surface damage area in images of implants lit by indirect lighting (rather than trans-illumination).^{23,24} The primary improvements of the method presented here included the use of trans-illumination (rather than indirect lighting) to highlight subsurface features while rendering surface damage less visible, and the development of an automated damage measurement method rather than hand-tracing. In this study, application of the measurement technique was limited by the result that only one specimen exhibited relevant damage.

Previous researchers using intermediate-complexity wear tests have generated more abundant damage and spalling, extending to several millimeters of depth, in aged, radiation-sterilized UHMWPE specimens.^{8,10,12,15,16} The GUR 4150 and GUR 1050 materials examined in all of those previous studies have molecular weights of $\sim 6 \times 10^6 \text{ g mol}^{-1}$, which is greater than the $\sim 3.5 \times 10^6 \text{ g mol}^{-1}$ molecular weight of the GUR 1020 material in the wear test of the present study.²⁵ Moreover, GUR 4150 is no longer used for orthopedic implants, in part because of suspicions that its processing additive, calcium stearate, may impair fusion of the raw material powder and facilitate fatigue damage.²⁵ The lower molecular weight of GUR 1020 comes with fewer molecular entanglements,²⁶ which makes the material more ductile.²⁷ This may partly explain why, in spite of being radiation-sterilized and subsequently aged, the GUR 1020 did not spall in this study. The near-surface location of the

damage is a novel observation, and it provides impetus for further study of the materials and development of the test method: a study comparing GUR 1050 with GUR 1020 is suggested. Another important consideration for long-term testing is the potential of *in vivo* fluids to contribute to oxidative degradation of UHMWPE.²⁸

Articulation of a convex-concave knee condyle contact pair normally requires a multi-dimensional motion trajectory which includes repetitive cross shear in order not to attenuate the wear modes known as most damaging in total knee replacement implants. Using a surrogate contact pair to simplify the UHMWPE surface to a plane can simplify the trajectory to 2D, while nonetheless closely mimicking the contact mechanics of a corresponding full-scale condyle pair. The repetitive contact stresses elicited during a select, critical segment of a normal gait cycle could be replicated with high fidelity using simple surrogate contact pairs in a wear test apparatus that is far less complicated than a knee joint simulator. This would pave the way to efficient high-cycle durability testing of UHMWPE under contact stress conditions that accurately mimic those of a specific design of a knee condyle contact pair. In any such simplified wear testing of UHMWPE, it is important to use motion paths that elicit multidirectional shear stresses, as caused in this test by the overlapping contact areas from opposite sides of the square wear track. In this study, the subject of investigation was a posterior-stabilized knee; yet, in principal, any condylar design can be represented with the same general type of surrogate contact pair. Combined with the opportunity to execute the test method on already-available equipment rather than custom-made rigs, this makes the method well-suited to standardization, which would provide a level basis for comparing the high-cycle durability of various designs and materials as a design tool, prior to screening final implant designs on knee simulators for safety and regulatory verification.

CONCLUSION

We have developed a wear test method of intermediate complexity that represents knee condyle contact stresses much more accurately than a simple POD test setup would, while avoiding the major complexity of a knee joint simulator. To achieve this, we implemented a validated theory for designing an accurate surrogate contact pair, in a wear test that can be executed in a standard, widely available, multi-station test machine. Further, we developed a digital imaging and processing technique for quantifying fatigue-type damage in the UHMWPE. We anticipate that the newly developed techniques will be useful for comparing the high-cycle durability of the most advanced UHMWPE types against one another—in a standardized method inclusive of the design-specific contact stresses of prosthetic knees—rather than against older, outmoded materials.

ACKNOWLEDGMENTS

The authors thank Howard Bush of Orchid Chelsea, Carlyle Creger of IMDS, and Tyler Bushman of Accutech Machining for manufacturing the test specimens, and Joe Lucero of Ortho Development for their CMM measurements.

REFERENCES

- Health, United States, 2011. National Center for Health Statistics. Hyattsville, Maryland. 2012. Available at: URL: <http://www.cdc.gov/nchs/hus/contents2011.htm#022>. Accessed on November 20, 2012.
- ISO 14243-1: Implants for surgery—Wear of total knee-joint prostheses. Part 1: Loading and displacement parameters for wear-testing machines with load control and corresponding environmental conditions for test. International Organization for Standardization. Geneva, Switzerland. 2009.
- ISO 14242-1: Implants for surgery—wear of total hip-joint prostheses. Part 1: Loading and displacement parameters for wear-testing machines and corresponding environmental conditions for test. International Organization for Standardization. Geneva, Switzerland. 2002.
- Schmalzried TP, Szuszczewicz ES, Northfield MR, Akizuki KH, Frankel RE, Belcher G, Amstutz HC. Quantitative assessment of walking activity after total hip or knee replacement. *J Bone Joint Surg Am* 1998;80:54–59.
- Morlock M, Schneider E, Bluhm A, Vollmer M, Bergmann G, Muller V, Honl M. Duration and frequency of every day activities in total hip patients. *J Biomech* 2001;34:873–881.
- Haider H. Tribological assessment of UHMWPE in the knee. In: Kurtz SM, editor. *UHMWPE Biomaterials Handbook*, 2nd ed. Burlington, MA: Academic Press; 2009. pp 381–408.
- Bragdon CR, O'Connor DO, Lowenstein JD, Jasty M, Biggs SA, Harris WH. A new pin-on-disk wear testing method for simulating wear of polyethylene on cobalt-chrome alloy in total hip arthroplasty. *J Arthroplasty* 2001;16:658–665.
- Currier JH, Duda JL, Sperling DK, Collier JP, Currier BH, Kennedy FE. In vitro simulation of contact fatigue damage found in ultra-high molecular weight polyethylene components of knee prostheses. *Proc Inst Mech Eng H* 1998;212:293–302.
- Chyr A, Sanders AP, Raeymaekers B. A hybrid apparatus for friction and accelerated wear testing of total knee replacement bearing materials. *Wear* 2013;308:54–60.
- Walker PS, Blunn GW, Lilley PA. Wear testing of materials and surfaces for total knee replacement. *J Biomed Mater Res* 1996;33:159–175.
- Muratoglu OK, Bragdon CR, O'Connor DO, Jasty M, Harris WH, Gul R, McGarry F. Unified wear model for highly crosslinked ultra-high molecular weight polyethylenes (UHMWPE). *Biomaterials* 1999;20:1463–1470.
- Reeves EA, Barton DC, Fitzpatrick DP, Fisher J. Comparison of gas plasma and gamma irradiation in air sterilization on the delamination wear of the ultra-high molecular weight polyethylene used in knee replacements. *Proc Inst Mech Eng H* 2000;214:249–255.
- Saikko V, Caloni O. Simulation of wear rates and mechanisms in total knee prostheses by ball-on-flat contact in a five-station, three-axis test rig. *Wear* 2002;253:424–429.
- Yao JQ, Blanchard CR, Lu X, Laurent MP, Johnson TS, Gilbertson LN, Swarts DF, Crowninshield RD. Improved resistance to wear, delamination and posterior loading fatigue damage of electron beam irradiated, melt-annealed, highly crosslinked UHMWPE knee inserts. In: Kurtz SM, Gsell RA, Martell J, editors. *Cross-linked and Thermally Treated Ultra-High Molecular Weight Polyethylene for Joint Replacements: ASTM STP 1445*. West Conshohocken, PA: ASTM International; 2003. pp 59–72.
- Van Citters DW, Kennedy FE, Currier JH, Collier JP, Nichols TD. A multi-station rolling/sliding tribotester for knee bearing materials. *J Tribol* 2004;126:380–385.
- Maher SA, Furman BD, Babalola OM, Cottrell JM, Wright TM. Effect of crosslinking, remelting, and aging on UHMWPE damage in a linear experimental wear model. *J Orthop Res* 2007;25:849–857.
- Richter BI, Ostermeier S, Turger A, Denkena B, Hurschler C. A rolling-gliding wear simulator for the investigation of tribological material pairings for application in total knee arthroplasty. *Biomed Eng Online* 2010;9:24.
- Morra EA, Greenwald AS. Polymer insert stress in total knee designs during high-flexion activities: A finite element study. *J Bone Joint Surg Am* 2005;87:120–124.
- Kennedy FE, Currier JH, Plumet S, Duda JL, Gestwick DP, Collier JP, Currier BH, Duborg M-C. Contact fatigue failure of ultra-high molecular weight polyethylene bearing components of knee prostheses. *J Tribol* 2000;122:332–339.
- Sanders AP, Brannon RM. Determining a surrogate contact pair in a Hertzian contact problem. *J Tribol* 2011;133:024502–024506.
- Sanders AP, Brannon RM. Assessment of the applicability of the Hertzian contact theory to edge-loaded prosthetic hip bearings. *J Biomech* 2011;44:2802–2808.
- Muratoglu OK, Bragdon CR, Jasty M, O'Connor DO, Von Knoch RS, Harris WH. Knee-simulator testing of conventional and cross-linked polyethylene tibial inserts. *J Arthroplasty* 2004;19:887–897.
- Cornwall GB, Bryant JT, Hansson CM, Rudan J, Kennedy LA, Cooke TDV. A quantitative technique for reporting surface degradation patterns of UHMWPE components of retrieved total knee replacements. *J Appl Biomater* 1995;6:9–18.
- Harman MK, Banks SA, Hodge WA. Polyethylene damage and knee kinematics after total knee arthroplasty. *Clin Orthop* 2001;392:383–393.
- Kurtz SM. From ethylene gas to UHMWPE component: The process of producing orthopedic implants. In: Kurtz SM, editor. *UHMWPE Biomaterials Handbook*, 2nd ed. Burlington, MA: Academic Press; 2009. pp 7–19.
- Ferry JD. *Viscoelastic Properties of Polymers*, 3rd ed. United States of America: Wiley; 1980.
- Greer KW, King RS, Chan FW. The effects of raw material, irradiation dose, and irradiation source on crosslinking of UHMWPE. In: Kurtz SM, Gsell RA, Martell J, editors. *STP 1445: Crosslinked and Thermally Treated Ultra-High Molecular Weight Polyethylene for Joint Replacements*. West Conshohocken, PA: ASTM International; 2004. pp 209–220.
- Oral E, Ghali BW, Neils A, Muratoglu OK. A new mechanism of oxidation in ultrahigh molecular weight polyethylene caused by squalene absorption. *J Biomed Mater Res B Appl Biomater* 2012, 100:742–751.